Stochastic Acoustic Ray Tracing with Dynamically Orthogonal Differential Equations

M.J. Humara[a], W.H. Ali[a], A. Charous[a], M. Bhabra[a], P.F.J. Lermusiaux[a†]
[a] *Department of Mechanical Engineering, Massachusetts Institute of Technology, Cambridge, MA*
[†]Corresponding Author: pierrel@mit.edu

OCEANS 2022, Hampton Roads | 978-1-6654-6809-1/22/$31.00 ©2022 IEEE | DOI: 10.1109/OCEANS47191.2022.9977252

***Abstract*—Developing accurate and computationally efficient models for underwater sound propagation in the uncertain, dynamic ocean environment is inherently challenging. In this work, we evaluate the potential of dynamic reduced-order modeling for stochastic ray tracing. We obtain and implement the stochastic dynamically-orthogonal (DO) differential equations for Ray Tracing (DO-Ray). With stochastic DO-Ray, we can start from non-Gaussian environmental uncertainties and compute the stochastic acoustic ray fields in a dynamic reduced order fashion, all while preserving the dominant complex statistics of the ocean environment and the nonlinear relations with ray dynamics. We develop varied algorithms and discuss implementation challenges and solutions, using direct Monte Carlo for comparison. We showcase results in an uncertain deep-sound channel example and observe the ability to represent the stochastic ray trace fields in a dynamic reduced-order fashion.**

***Index Terms*—Underwater acoustics, probabilistic ray tracing, stochastic ODEs, ocean forecasting, tomography, travel time, data assimilation**

I. Introduction

Developing accurate and computationally efficient models for ocean acoustics is inherently challenging due to several factors including the complex physical processes and the need to provide results on a large range of scales [1–4]. Furthermore, the ocean itself is an inherently dynamic environment within the multiple scales [5, 6]. Even if we could measure the exact properties at a specific instant, the ocean will continue to change in the smallest temporal scales, ever increasing the uncertainty in the ocean prediction and affecting acoustic performance prediction [7, 8].

In this work, we evaluate the potential of Reduced-Order Models for stochastic ocean acoustics prediction. We derive and implement the stochastic DO differential equations for Ray Tracing (DO-Ray), starting from the differential equations of Ray theory. With a stochastic DO-Ray implementation, we can start from non-Gaussian environmental uncertainties and compute the stochastic acoustic ray fields in a reduced order fashion, all while preserving the complex statistics of the ocean environment and the nonlinear relations with stochastic ray tracing. We present the stochastic DO-Ray methodology, develop varied algorithms, and discuss implementation challenges and solutions, using direct Monte Carlo for comparison. We apply the DO-Ray methodology to stochastic sound-speed profiles (SSPs), an idealized uncertain deep-sound channel. Our results confirm the ability to represent the stochastic ray trace field in a reduced order fashion, including non-Gaussian statistics.

The present work in stochastic DO-Ray follows contributions in stochastic modeling for underwater acoustics in an uncertain ocean environment [8–10]. Related progress in stochastic underwater acoustics includes Monte Carlo sampling [11–14], Error Subspace Statistical Estimation with ensemble schemes [15–19], and Polynomial Chaos equations [20–24] techniques. However, large number of realizations and expansion coefficients are typically required to capture the multi-dimensional environmental uncertainties making these techniques computationally infeasible [25]. More recently, DO-based techniques have been proposed to efficiently capture the environmental uncertainties and predict the resulting acoustic fields and their probability distributions. These include the DO parabolic equations [26, 27], the DO wave equations [28], and the reduced-order deterministic 3D parabolic equations [28].

II. Problem Statement

The governing equations for acoustic ray tracing are [2, 5]:

$$\frac{d\boldsymbol{\xi}(s)}{ds} = -\frac{1}{c(\mathbf{x})^2}\nabla c(\mathbf{x}) \tag{1}$$

$$\frac{d\mathbf{x}(s)}{ds} = c(\mathbf{x})\boldsymbol{\xi}(s)\,. \tag{2}$$

where $\boldsymbol{\xi}(s)$ and $\mathbf{x}(s)$ determine the ray trajectories parametrized by the arc length s, and $c(\mathbf{x})$ is the sound speed along the ray trajectory. Equations (1) and (2) are a coupled system of first-order ODEs. The initial condition for $\mathbf{x}$ is self-evident as we consider a ray starting at $\mathbf{x}_0 = \langle x_1 = 0, x_2 = depth \rangle$ given an initial launch angle θ_0, in an acoustic medium described by $c(\mathbf{x})$, taking a step of length ds. The direction a ray travels as it marches along its arc length is $\frac{d\mathbf{x}}{ds}$. We can thus rearrange equation (2) to establish the following initial conditions for an individual ray's components $\mathbf{x}$ and $\boldsymbol{\xi}$:

$$\boldsymbol{\xi}_0 = \begin{bmatrix} \frac{\cos\theta_0}{c(\mathbf{x}_0)} \\ \frac{\sin\theta_0}{c(\mathbf{x}_0)} \end{bmatrix} \;;\; \mathbf{x}_0 = \begin{bmatrix} 0 \\ \text{Source Depth} \end{bmatrix}. \tag{3}$$

Furthermore, the boundary conditions for equations (1) and (2) are discussed in [5].

We now combine Ray Tracing with Dynamically Orthogonal (DO) Equations [29–32] for stochastic acoustic computation. We start by explaining the intuition provided by Figure 1.

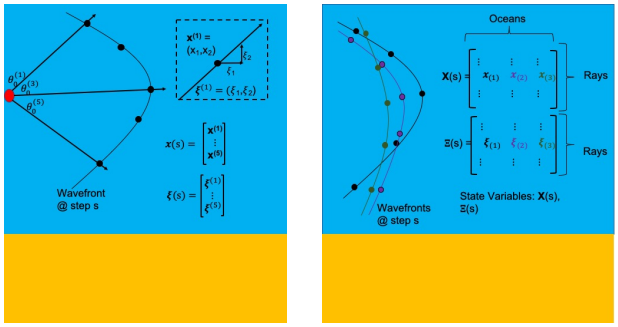

(a) Single Ocean Wavefront Realization at step "s."

(b) Multiple Ocean Wavefront Realizations at step "s."

Fig. 1: (a) Depiction of how for a single ocean, the wavefront at a given step along all of the rays "s" can be represented by 2 vectors, each of length $2 \times$ (*#rays*). (b) Depiction at the same step along the rays "s," for multiple ocean realizations, $\mathbf{X}$ and $\mathbf{\Xi}$ represent a field of wavefronts for which we can obtain a reduced order representation.

For the reduced-order DO representation (in Einstein notation) of the stochastic ocean acoustics fields, $\mathbf{X}$ and $\mathbf{\Xi}$, we proceed as follows. We characterize each individual ocean realization, essentially a sound speed field realization, as the sum of the mean of the ocean fields with a linear combination of the number of modes determined necessary to capture the variability in the fields multiplied by their respective stochastic coefficients [26, 33].

Due to the stochastic sound-speed field, the underwater sound propagation field will also be stochastic. We decompose the acoustic rays state variables using a DO decomposition, specifically:

$$\mathbf{x}(s;\eta) = \overline{\mathbf{x}}(s) + \tilde{\mathbf{x}}_i(s)\beta_i(s;\eta) \tag{4}$$

$$\boldsymbol{\xi}(s;\eta) = \overline{\boldsymbol{\xi}}(s) + \tilde{\boldsymbol{\xi}}_i(s)\gamma_i(s;\eta) \tag{5}$$

The subscript "i" pertain to the DO modes and "η" pertains to a particular ocean realization event, and the summation over all "i" is implied.

The most straightforward and simplest method to obtain wavefront realizations is through a Monte Carlo implementation, hence solving for each ocean realization in series or parallel. A DO-Ray methodology allows for computing these realizations using a reduced representation of the stochastic field by solving governing ODEs for the stochastic mean $(\overline{\mathbf{x}}(s), \overline{\boldsymbol{\xi}}(s))$, DO modes $(\tilde{\mathbf{x}}_i(s), \tilde{\xi}_i(s))$, and DO coefficients $(\beta_i(s;\eta), \gamma_i(s;\eta))$.

Up to this point, we have discussed why stochastic acoustic computation is relevant and why a Monte Carlo approach could present computational challenges. We are hinging the ability of our algorithm's computational accuracy on the presumption that we can represent the variation of a field of ray traces, each corresponding to a specific ocean realization, with a reduced-order representation of DO modes and coefficients. Such an approach and corresponding results have been shown to be very efficient for acoustic parabolic PDEs [26, 27, 34]. For the present novel DO-ray approach, an empirical assessment to evaluate if the stochastic ray trace field can be reduced using a dynamic reduced-order approach is completed in [35], along with a convergence study with the number of DO modes.

In what follows, we derive the DO equations for ray tracing, and summarize the DO-Ray algorithms discussed in [35]. We also study some of the new computational intricacies that we introduce with a DO-Ray implementation. We examine the opportunities for further reduction in our representation, as well as some of the inherent challenges of the implementation. Lastly we analyze the computational cost of our DO-Ray implementation.

III. Methodology

The DO-Ray differential equations can be obtained by inserting the truncated decompositions from equations (4) and (5) in the governing ray equations (1) and (2). For simplicity, when annotating state variables or ocean realizations, we do not always include the dependent variable. It is useful to introduce the following concepts:

- When we use the term stochastic fields ($\mathbf{X}$ and $\mathbf{\Xi}$), we consider multiple realizations, typically O(10^3–10^4) and possibly much more, with each realization characterized by an ($\mathbf{x}$, $\boldsymbol{\xi}$) pair forming a column of the matrices $\mathbf{X}$ and $\mathbf{\Xi}$. After subtracting the mean of all realizations, we perform a singular value decomposition to obtain the DO modes and coefficients.
  - For example, $\mathbf{U\Sigma V}^T = svd(\mathbf{X} - \mathbb{E}^{\eta}[\mathbf{X}])$, where the DO modes $\tilde{\mathbf{x}}$ are the columns of $\mathbf{U}$, and the DO coefficients, corresponding to a particular realization, are the rows of $\mathbf{\Sigma V}^T$.
- Realizations of stochastic state variables $\boldsymbol{\xi}(s;\eta)$ and $\mathbf{x}(s;\eta)$ dependent on "s" and correspond to a particular ocean realization. They also have their stochastic representations for a particular realization "η":
  $\boldsymbol{\xi}(s;\eta) \equiv \boldsymbol{\xi} = \overline{\boldsymbol{\xi}} + \tilde{\boldsymbol{\xi}}_i\gamma_i$
  $\mathbf{x}(s;\eta) \equiv \mathbf{x} = \overline{\mathbf{x}} + \tilde{\mathbf{x}}_i\beta_i$
- The stochastic means and DO modes are only a function of "s":
  $\overline{\boldsymbol{\xi}}_i(s) \equiv \overline{\boldsymbol{\xi}}_i$ and $\tilde{\boldsymbol{\xi}}_i(s) \equiv \tilde{\boldsymbol{\xi}}_i$
  $\overline{\mathbf{x}}(s) \equiv \overline{\mathbf{x}}$ and $\tilde{\mathbf{x}}_i(s) \equiv \tilde{\mathbf{x}}_i$
- The DO coefficients are dependent on "η" and correspond to a particular ocean realization:
  $\gamma_i(s;\eta) \equiv \gamma_i$
  $\beta_i(s;\eta) \equiv \beta_i$

- The sound speed along a stochastic ray depends on position $\mathbf{x}(s;\eta)$ and on the ocean realization:
$$c(\mathbf{x}(s;\eta);\eta) \equiv c(\mathbf{x})$$

A. Evolution of the Stochastic Mean $\left(\frac{d\bar{\boldsymbol{\xi}}(s)}{ds}, \frac{d\bar{\mathbf{x}}(s)}{ds}\right)$

We begin with the stochastic versions of (1) and (2). Inserting the decompositions (4) and (5), we obtain:

$$\begin{aligned}\frac{d}{ds}(\bar{\boldsymbol{\xi}} + \tilde{\boldsymbol{\xi}}_i\gamma_i) &= -\frac{1}{c(\mathbf{x})^2}\nabla c(\mathbf{x}) \\ \frac{d}{ds}(\bar{\mathbf{x}} + \tilde{\mathbf{x}}_i\beta_i) &= c(\mathbf{x})\boldsymbol{\xi}\end{aligned} \tag{6}$$

We then take the expectation ($\mathbb{E}^\eta$) over all ocean realizations, and obtain:

$$\begin{aligned}\frac{d\bar{\boldsymbol{\xi}}}{ds} &= \mathbb{E}^\eta\left[-\frac{1}{c(\mathbf{x})^2}\nabla c(\mathbf{x})\right] \\ \frac{d\bar{\mathbf{x}}}{ds} &= \mathbb{E}^\eta\left[c(\mathbf{x})\boldsymbol{\xi}\right]\end{aligned} \tag{7}$$

to describe how the stochastic mean of the acoustic ray trace field propagates.

B. Evolution of the DO Coefficients $\left(\frac{d\gamma_i(s;\eta)}{ds}, \frac{d\beta_i(s;\eta)}{ds}\right)$

Starting again with (6), we subtract (7) and take the projection onto $\tilde{\boldsymbol{\xi}}_j(s)$ and $\tilde{\mathbf{x}}_j(s)$, respectively, to obtain:

$$\begin{aligned}&\frac{d\gamma_i}{ds}\langle\tilde{\boldsymbol{\xi}}_i, \tilde{\boldsymbol{\xi}}_j\rangle + \gamma_i\left\langle\frac{d\tilde{\boldsymbol{\xi}}_i}{ds}, \tilde{\boldsymbol{\xi}}_j\right\rangle = \\ &\left\langle -\frac{1}{c(\mathbf{x})^2}\nabla c(\mathbf{x}) - \mathbb{E}^\eta\left[-\frac{1}{c(\mathbf{x})^2}\nabla c(\mathbf{x})\right], \tilde{\boldsymbol{\xi}}_j\right\rangle, \\ &\frac{d\beta_i}{ds}\langle\tilde{\mathbf{x}}_i, \tilde{\mathbf{x}}_j\rangle + \beta_i\left\langle\frac{d\tilde{\mathbf{x}}_i}{ds}, \tilde{\mathbf{x}}_j\right\rangle = \\ &\left\langle c(\mathbf{x})\boldsymbol{\xi} - \mathbb{E}^\eta\left[c(\mathbf{x})\boldsymbol{\xi}\right], \tilde{\mathbf{x}}_j\right\rangle.\end{aligned} \tag{8}$$

Applying the DO condition, we obtain:

$$\begin{aligned}\frac{d\gamma_j}{ds} &= \left\langle -\frac{1}{c(\mathbf{x})^2}\nabla c(\mathbf{x}) - \mathbb{E}^\eta\left[-\frac{1}{c(\mathbf{x})^2}\nabla c(\mathbf{x})\right], \tilde{\boldsymbol{\xi}}_j\right\rangle, \\ \frac{d\beta_j}{ds} &= \left\langle c(\mathbf{x})\boldsymbol{\xi} - \mathbb{E}^\eta\left[c(\mathbf{x})\boldsymbol{\xi}\right], \tilde{\mathbf{x}}_j\right\rangle,\end{aligned} \tag{9}$$

to describe the evolution of the DO coefficients.

C. Evolution of the DO Modes $\left(\frac{d\tilde{\boldsymbol{\xi}}_i(s)}{ds}, \frac{d\tilde{\mathbf{x}}_i(s)}{ds}\right)$

Starting again with (6), we project onto the stochastic space by multiplying with the stochastic DO coefficients (γ_k,β_k) and take the expectation. We then use the prior equations to obtain:

$$\begin{aligned}\frac{d\tilde{\boldsymbol{\xi}}_i}{ds} &= \left[\mathbb{E}^\eta\left[-\frac{\gamma_k}{c(\mathbf{x})^2}\nabla c(\mathbf{x})\right] - \right. \\ &\mathbb{E}^\eta\left[\left\langle -\frac{1}{c(\mathbf{x})^2}\nabla c(\mathbf{x}) - \right.\right. \\ &\left.\left.\mathbb{E}^\eta\left[-\frac{1}{c(\mathbf{x})^2}\nabla c(\mathbf{x})\right], \tilde{\boldsymbol{\xi}}_j\right\rangle\gamma_k\right]\tilde{\boldsymbol{\xi}}_i\Bigg]\mathbb{E}^\eta[\gamma_i\gamma_k]^{-1}, \\ \frac{d\tilde{\mathbf{x}}_i}{ds} &= \left[\mathbb{E}^\eta\left[c(\mathbf{x})\boldsymbol{\xi}\beta_k\right] - \right. \\ &\left.\mathbb{E}^\eta\left[\left\langle c(\mathbf{x})\boldsymbol{\xi} - \mathbb{E}^\eta\left[c(\mathbf{x})\boldsymbol{\xi}\right], \tilde{\mathbf{x}}_j\right\rangle\beta_k\right]\tilde{\mathbf{x}}_i\right]\mathbb{E}^\eta[\beta_i\beta_k]^{-1},\end{aligned} \tag{10}$$

to describe the evolution of the DO modes.

D. Stochastic DO-Ray Algorithms and Reduced-Order Representations

We now first write the previously derived DO equations in a realization matrix form.

1) Matrix Representations: Prior to computing and evolving the stochastic field, we select two computational parameters from which we will construct a reduced representation:

- the number of rays, R, used to form the ray trace,
- the number of DO modes, M, necessary to capture the variation between the H (# of oceans) different traces.

Here we define the matrices used in the DO-Ray equations and specify the dimensions of each:

- $\mathbf{X}$ is comprised of all ray positions for all realizations at a particular range-step s. $\mathbf{X}_r$ and $\mathbf{X}_d$ correspond to range and depth components respectively. Both $\mathbf{X}_r$ and $\mathbf{X}_d$ are $R \times H$ size matrices. Similarly $\boldsymbol{\Xi}$ is comprised of all $\boldsymbol{\xi}$ for all realizations at a particular step along the ray. $\boldsymbol{\Xi}_r$ and $\boldsymbol{\Xi}_d$ correspond to range and depth components respectively. Both $\boldsymbol{\Xi}_r$ and $\boldsymbol{\Xi}_d$ are $R \times H$ size matrices.
- Both $\mathbf{X}$ and $\boldsymbol{\Xi}$ can be decomposed into their respective means, DO modes, and DO coefficients for a particular range-step "s".
$$\begin{aligned}\mathbf{X}_{r,d} &= \bar{\mathbf{x}}_{r,d} + \tilde{\mathbf{X}}_{r,d}B \\ \boldsymbol{\Xi}_{r,d} &= \bar{\boldsymbol{\xi}}_{r,d} + \tilde{\boldsymbol{\Xi}}_{r,d}\Gamma\end{aligned}$$
- The range and depth components of $\bar{\boldsymbol{\xi}}_{r,d}$ and $\bar{\mathbf{x}}_{r,d}$ are vectors of length R.
- DO mode matrices: $dim(\tilde{\mathbf{X}}_{r,d}) = R \times M$; $dim(\tilde{\boldsymbol{\Xi}}_{r,d}) = R \times M$.
- DO coefficient matrices: $dim(B) = dim(\Gamma) = M \times H$
- $\mathbf{C} = c_{\eta=1:H}(\mathbf{X})$; $dim(\mathbf{C}) = R \times H$.
- $\mathbf{C}_x = \frac{1}{c^2_{\eta=1:H}(\mathbf{X})}$; $dim(\mathbf{C}_x) = R \times H$.

- $\nabla_{r,d}\mathbf{C} = \nabla_{r,d}C(\mathbf{X})$, where ∇_r and ∇_d represent the range and depth components of the gradients respectively. $dim(\nabla_{r,d}\mathbf{C}) = R \times H$

2) Evolution of the DO Means: From Equation (7) we can put the equation in matrix form:

$$\frac{d\overline{\mathbf{x}}_{r,d}}{ds} = \mathbb{E}^{\eta}\left[\mathbf{C}.*(\overline{\boldsymbol{\xi}}_{r,d} + \tilde{\boldsymbol{\Xi}}_{r,d}\Gamma)\right] \tag{11}$$

and

$$\frac{d\overline{\xi}_{r,d}}{ds} = \mathbb{E}^{\eta}\left[\mathbf{C}.*\nabla_{r,d}\mathbf{C}\right] \tag{12}$$

3) Evolution of the DO Coefficients: From Equation (9):

$$\begin{aligned}\frac{d}{ds}[B] = \tilde{\mathbf{X}}_r^T\big(\mathbf{C}.*\overline{\boldsymbol{\xi}_r} + \mathbf{C}.*(\tilde{\boldsymbol{\Xi}}_r\Gamma) - \frac{d\overline{\mathbf{x}_r}}{ds}\big)\\ + \tilde{\mathbf{X}}_d^T\big(\mathbf{C}.*\overline{\boldsymbol{\xi}_d} + \mathbf{C}.*(\tilde{\boldsymbol{\Xi}}_d\Gamma) - \frac{d\overline{\mathbf{x}_d}}{ds}\big)\end{aligned} \tag{13}$$

and

$$\begin{aligned}\frac{d}{ds}[\Gamma] = \tilde{\boldsymbol{\Xi}}_r^T\big(-\mathbb{E}^{\eta}\big[\mathbf{C}_x.*\nabla_r\mathbf{C}\big] - \mathbf{C}_x.*\nabla_r\mathbf{C}\big)\\ + \tilde{\boldsymbol{\Xi}}_r^T\big(-\mathbb{E}^{\eta}\big[\mathbf{C}_x.*\nabla_d\mathbf{C}\big] - \mathbf{C}_x.*\nabla_d\mathbf{C}\big)\end{aligned} \tag{14}$$

4) Evolution of the DO Modes: From Equation (10):

$$\begin{aligned}\frac{d\tilde{\mathbf{X}}_r}{ds} &= \left[\frac{1}{\eta}\mathbf{C}_x.*(\overline{\boldsymbol{\xi}}_r + \tilde{\boldsymbol{\Xi}}_r\Gamma)B^T\right.\\ &\left. - \tilde{\mathbf{X}}_r\left(\frac{1}{\eta}\left(\frac{dB}{ds}B^T\right)\right)\right]Cov\big\{B^T\big\}^{-1}\\ \frac{d\tilde{\mathbf{X}}_d}{ds} &= \left[\frac{1}{\eta}\mathbf{C}_x.*(\overline{\boldsymbol{\xi}}_d + \tilde{\boldsymbol{\Xi}}_d\Gamma)B^T -\right.\\ &\left.\tilde{\mathbf{X}}_d\left(\frac{1}{\eta}\left(\frac{dB}{ds}B^T\right)\right)\right]Cov\big\{B^T\big\}^{-1}\end{aligned} \tag{15}$$

and

$$\begin{aligned}\frac{d\tilde{\boldsymbol{\Xi}}_r}{ds} &= \left[\frac{1}{H}\big((\mathbf{C}_x.*\nabla_r\mathbf{C})\Gamma^T\big) -\right.\\ &\left.\tilde{\boldsymbol{\Xi}}_r\left(\frac{1}{H}\left(\frac{d\Gamma}{ds}\Gamma^T\right)\right)\right]Cov\big\{\Gamma^T\big\}^{-1}\\ \frac{d\tilde{\boldsymbol{\Xi}}_d}{ds} &= \left[\frac{1}{H}\big((\mathbf{C}_x.*\nabla_d\mathbf{C})\Gamma^T\big) -\right.\\ &\left.\tilde{\boldsymbol{\Xi}}_d\left(\frac{1}{H}\left(\frac{d\Gamma}{ds}\Gamma^T\right)\right)\right]Cov\big\{\Gamma^T\big\}^{-1}\end{aligned} \tag{16}$$

5) Reduced Order Representation of the Nonlinear Stochastic SSP along Stochastic Acoustic Rays: Now that we see the discrete matrix-form DO-Ray evolution equations, it is apparent that though we have reduced representations of the acoustic field, the computational cost can be higher with a DO-Ray computation as compared to a Monte Carlo approach. Hence, we now delve into why our present DO-Ray implementation can be less efficient than a direct Monte-Carlo scheme. Later, we provide ideas on how this can be remedied.

At each step in the evolution, we presently compute the sound-speed for each individual ray, for all ocean realizations, at every step ($H \times R$ computations). This inefficiency exists for both Monte-Carlo and DO implementations; however, where we gained efficiency in reducing our representation of the stochastic field, in the above implementation, we lose some efficiency in having to reconstitute all realizations in order to evaluate the sound speeds for the next step along each advancing ray. It is important to understand why we cannot obtain the additional reduction in the sound-speed distribution with the above equations, in order to provide guidance on how one may be able to increase efficiency in future work.

Consider an arbitrary distribution of SSP measurements for which we can form functions $c_{1:H}(\mathbf{x})$. As we decompose the stochastic fields of the acoustic ray state variables, we could decompose c into its mean, DO modes and coefficients:

$$c(\mathbf{x}(s;\eta);\eta) = \overline{c}(\mathbf{x}(s;\eta)) + \tilde{c}_j(\mathbf{x}(s;\eta))\alpha_j(\eta) \tag{17}$$

where our stochastic location field $\mathbf{x}$ along a stochastic ray is both a function of the step along the ray and of the ocean realization. Presently, the sound speed profiles are frozen in time and are only dependent on the realization selected and spatial location. Inserting the stochastic representations of $\mathbf{x}$ in (17), we have:

$$\begin{aligned}c(\overline{\mathbf{x}} + \tilde{\mathbf{x}}_i\beta_i(\eta);\eta) =& \overline{c}(\overline{\mathbf{x}} + \tilde{\mathbf{x}}_i\beta_i(\eta)) +\\ & \tilde{c}_j(\overline{\mathbf{x}} + \tilde{\mathbf{x}}_i\beta_i(\eta))\,\alpha_j(\eta)\,.\end{aligned} \tag{18}$$

To exemplify the computational issues involved with the nonlinear evaluation of the stochastic sound-speed along stochastic rays, we discuss the evolution of the stochastic mean (7) with the added reduced order in $c_{1:H}(\mathbf{x})$. We start by inserting (18) into (6) and take the expectations over all ocean realizations to obtain the revised RHS of (7):

$$\begin{aligned}&LHS_{\boldsymbol{\xi}} =\\ &\mathbb{E}^{\eta}\Bigg[-\frac{1}{\Big(\overline{c}(\overline{\mathbf{x}} + \tilde{\mathbf{x}}_i\beta_i(\eta)) + \tilde{c}_j(\overline{\mathbf{x}} + \tilde{\mathbf{x}}_i\beta_i(\eta))\alpha_j(\eta)\Big)^2}\\ &\nabla\Big(\overline{c}(\overline{\mathbf{x}} + \tilde{\mathbf{x}}_i\beta_i(\eta)) + \tilde{c}_j(\overline{\mathbf{x}} + \tilde{\mathbf{x}}_i\beta_i(\eta))\,\alpha_j(\eta)\Big)\Bigg]\,,\\ &LHS_{\mathbf{x}} =\\ &\mathbb{E}^{\eta}\Big[\Big(\overline{c}(\overline{\mathbf{x}} + \tilde{\mathbf{x}}_i\beta_i(\eta)) + \tilde{c}_j(\overline{\mathbf{x}} + \tilde{\mathbf{x}}_i\beta_i(\eta))\,\alpha_j(\eta)\Big)\boldsymbol{\xi}(\eta)\Big]\,.\end{aligned} \tag{19}$$

Consider the latter equation of (19). Without going into the details of computing the RHS, we need to compute $\mathbb{E}^{\eta}\big[\big(\overline{c}(\overline{\mathbf{x}} + \tilde{\mathbf{x}}_i\beta_i(\eta)) + \tilde{c}_j(\overline{\mathbf{x}} + \tilde{\mathbf{x}}_i\beta_i(\eta))\,\alpha_j(\eta)\big)\boldsymbol{\xi}\big]$ or more simply $\mathbb{E}^{\eta}[c(\mathbf{x}(s;\eta);\eta)\boldsymbol{\xi}]$. Unless we have an equation that describes the functional relationship between the position and the sound speed along a particular ray, it

is challenging to compute this expectation over all realizations. There are a few approximations that we discuss next, with an increasing level of stochastic accuracy.

Local sound-speed mean approximation. First, we could make an approximation for the stochastic ray traces, with the most simple being $\overline{\mathbf{x}} + \tilde{\mathbf{x}}_i\beta_i \approx \overline{\mathbf{x}}$. With this approximation we arrive at:

$$c(\mathbf{x}(s;\eta);\eta) \approx \overline{c}(\overline{\mathbf{x}}) + \tilde{c}_j(\overline{\mathbf{x}})\alpha_j(\eta) \tag{20}$$

and thus $\mathbb{E}^\eta[c(\mathbf{x}(s;\eta);\eta)] \approx \mathbb{E}^\eta\left[\overline{c}(\overline{\mathbf{x}}) + \tilde{c}_j(\overline{\mathbf{x}})\alpha_j(\eta)\right]$. This zeroth-order stochastic approximation is similar to the assumption we made with the example application of EOFs in tomography in that we are assuming that perturbation in the rays across all realizations are relatively small. Therefore the sound-speed for all realizations is approximated as the sound speed for the mean profile plus a DO decomposition. Consider a distribution of constant positive sound speed profiles for which we have computed the mean profile. When considering the ray paths after some significant number of range steps the mean ray position may be a decent approximation and the sound-speed gradient exact as it is constant and positive.

Let's discuss this zeroth-order approximation of the sound-speed and imagine the situation where the sound speed has a probability distribution of constant both positive and negative sound speed gradients. Even though we have a better approximation to account for the ray path error in the different realizations, the effect of the sound speed gradients on the ray path, where the mean is no longer an accurate approximation, will result in inaccurate representations of how the ray will bend. Using the mean sound-speed gradient as an approximation results in an altered ray path as the gradients may have opposite signs.

It is feasible to construct scenarios under which this methodology could make the approximations above and reduce the computational cost of the DO-Ray methodology; however these could be overly specific and therefore are not considered in this thesis.

This illustrates an important point when considering the DO-Ray computational method based on the mean ocean only. The mean ray propagation in a non-Gaussian distribution could be nonphysical and is unlikely to approximate all of the realizations. We also note that the dynamics of the DO modes are only basis functions that describe the most variance and do not always correspond to specific acoustic physical process. They are intermediate computational quantities from which physical realizations can be reconstructed by linear combinations of the DO modes multiplied by the DO coefficients.

Local sound-speed Taylor-Series approximation. Second, if we were to deem that the error in ray position after the requisite number of steps would result in too large an error in sound-speed computation, we could consider consider first-order Taylor series expansion of the sound-speed functions around $\overline{\mathbf{x}}$ to better account for the difference in ray position:

$$c(\mathbf{x}) \approx c(\overline{\mathbf{x}}) + \nabla c(\overline{\mathbf{x}})(\mathbf{x} - \overline{\mathbf{x}}) \tag{21}$$

We can then apply such a first-order relation to the mean sound speed function and the DO modes function. This appears promising in that we have a representation of the $\mathbf{x} - \overline{\mathbf{x}}$ term: $\mathbf{x}_i\beta_i$. Hence, applying a first-order Taylor series expansion to both he sound-speed mean and the DO modes, our first-order stochastic approximation is:

$$c(\mathbf{x}) \approx \left(\overline{c}(\overline{\mathbf{x}}) + \nabla\overline{c}(\overline{\mathbf{x}})\tilde{\mathbf{x}}_i\beta_i\right) + \left(\tilde{c}_j(\overline{\mathbf{x}})\alpha_j + \nabla\tilde{c}_j(\overline{\mathbf{x}})\alpha_j\tilde{\mathbf{x}}_i\beta_i\right) \tag{22}$$

This is the first-order stochastic approximation. Similar relations can be derived for the other terms in the DO equations. Higher-order Taylor series can also be considered for additional accuracy in the stochastic space, but the computational costs of using such approximation quickly become large. In general, first-order and sometimes higher-order Taylor approximations have been very useful and efficient for stochastic DO energy-optimal and time-optimal path planning [36–40] as well as in stochastic biogeochemical modeling and inference [41]. We can expect that they would be also very useful for stochastic DO rays and this should be investigated.

Local sound-speed function. A third additional way to achieve the desired reduction to through other stochastic function approximation. However, it also results in a significant loss of generality and assumes knowledge of how the sound speed changes as a function of position on the ray as opposed to depth or position in the water column. Since the crux of the problem in evaluating the nonlinear $c(\mathbf{x}(s;\eta);\eta)$ is not knowing the analytical functional relationship and a simple (linear) representation, we could create an accurate but easy-to-deal with functional relationship with a stochastic dependency.

For instance, consider $\frac{dc(s)}{ds} = constant$, but assume the best approximation of the stochastic slope of the sound speed is to be determined ($m = \overline{m} + \alpha_j$). Instead of representing the stochastic sound-speed as $c(\mathbf{x};\eta) = \overline{c}(\mathbf{x}) + \tilde{c}_j(\mathbf{x})\alpha_j(\eta)$, we could represent it as:

$$c(\overline{\mathbf{x}} + \tilde{\mathbf{x}}_i\beta_i;\eta) = (\overline{m} + \alpha_j) * (\overline{\mathbf{x}} + \tilde{\mathbf{x}}_i\beta_i) + c_0 \tag{23}$$

Thus, considering the mean as an example,

$$\begin{aligned}\mathbb{E}^\eta[c(\mathbf{x}(s;\eta);\eta)] &= \mathbb{E}^\eta[(\overline{m} + \alpha_j) * (\overline{\mathbf{x}} + \tilde{\mathbf{x}}_i\beta_i) + c_0] \\ &= \overline{m}\overline{\mathbf{x}} + \tilde{\mathbf{x}}\mathbb{E}^\eta[\alpha_j\beta_i]\end{aligned} \tag{24}$$

The above equations could be optimized locally by least-squares (variance as for DO) or by clustering [42]. For equation (23), the result would remain a first-order approximation and be similar to the above first-order Taylor series approximation which was an expansion around the local range-dependent mean sound speed field.

Given an approximation for $c(s)$, we could extend this approach to any (higher-order) function that approximates

$c(s)$ locally and incorporate a stochastic term. Legendre polynomials can be used to approximate functions for sound speed; however, the computational expense and complexity increase with the increase of the order of polynomials required to accurately represent the SSPs. All all these approaches are related to local polynomial chaos expansion [43, 44], which can become very expensive if the order is increased and not so accurate if the stochastic fields to be approximated are dynamic and variable [43].

6) DO-Ray Computational Cost vs Monte Carlo: Consider a matrix form of governing ODEs (1) and (2):

$$\frac{d\mathbf{X}_{r,d}}{ds} = \mathbf{C}. * \mathbf{\Xi}_{r,d} \tag{25}$$

and

$$\frac{d\mathbf{\Xi}_{r,d}}{ds} = \mathbf{C}_x. * \nabla_{r,d}\mathbf{C}\,. \tag{26}$$

For a paralleled Monte Carlo approach, the number of floating point operations (FLOPS) to compute the RHS of any of the range or depth component matrices is $R \times H$ FLOPS. This is the exact same number of FLOPS in computing the value inside the expectation of (11) and (12), with the added number of FLOPS to recombine the mean, DO modes, and DO coefficients. Without even considering the cost of (13) through (16), since our present DO implementation does not use the efficient approximation of section III-D, the implementation is less efficient than Monte Carlo. To understand why, we start with an ODE of a form where where a DO implementation offers computational savings.

Consider an ODE of the form:

$$\frac{d\mathbf{X}}{ds} = A\mathbf{X} \tag{27}$$

as opposed to using the hadamard product $(.*)$ as in our computations, with A being a $R \times R$ matrix. The number of FLOPS to compute the RHS of (27) is $RH(R-1)$. If we represented $\mathbf{X}$ in a reduced form the computation of $A\bar{\mathbf{x}}$ and $A\tilde{\mathbf{X}}$ are $2R^2 - R$ and $2R^2M - RM$ respectively. Therefore computational savings is achievable if we can represent $\mathbf{X}$ with less than $\frac{H-2}{2}$ modes.

This appears to be a moot point, but we still consider why we cannot represent (26) and (27) in the form of (27). Consider $\mathbf{X}_r(s;\eta)$ consisting of R rays:

$$\begin{aligned} \frac{d\mathbf{X}_r}{ds} &= c(\mathbf{X})\mathbf{\Xi}_r; \\ c(\mathbf{X}) &= \begin{bmatrix} c_1(s) & & \\ & \ddots & \\ & & c_R(s) \end{bmatrix} \end{aligned} \tag{28}$$

In this case we could modify the equation to remove the hadamard product making $c(\mathbf{x})$ a diagonal matrix with the rays sound speed at step s along the diagonal for each ray. Observing the ODEs in this form illustrates why our present implementation will not provide computational savings, the computations do not rely on mutual information between rays.

Our use of a characteristic or Lagrangian approach when we discretized the wave-front to discrete rays traveling perpendicular to the wave, our derivation removed any correlation in space between the rays. Since each ray is computed independently without concern for its neighbors, we cannot directly achieve computational savings with the DO-Ray equations as implemented.

Based on the preceding paragraphs, it follows to ask, "Why is a DO-Ray approach is worth implementing?" Though in deriving the equations that would govern ray trajectories we removed the opportunity to capture ray inter-dependencies, that does not mean they are no longer present. As each ocean SSP will govern how a group of rays evolves, a Lagrangian approach allows us to see how the energy propagates with a certain number of rays to represent the field. We should be able to capture the majority of the information about our wavefront with a reduced representation of the rays. First, we could use the reductions discussed in section III-D. Second, we could utilize the wavefront information itself. We will indeed show that a low rank representation of the discretized wavefront can be marched in the ray domain ("s") and produce accurate representations of the stochastic field, even if more expensive in our present implementation. With this being possible, if we implement a DO wavefront or a modified DO-Ray scheme, we could use reduce the computational cost below that of Monte-Carlo.

7) Specific Stochastic DO-Ray Implementation: We now outline the specifics of how we implemented the stochastic DO-Ray equations. This outline will also further crystallize the above computational discussion. Since ultimately DO-Ray is compared to a Monte-Carlo implementation of the deterministic model, we list both.

For a Monte-Carlo integration of a determinisitc model with uncertain initial conditions, we assume that each ray is computed independently. The computation for all rays in all ocean realizations can then be computed in parallel. We refer to [35] for the algorithm.

Our present DO-Ray implementation for the stochastic reduced-order model computes all rays and realizations in parallel, but requires additional steps as outlined below:

- Perform Monte Carlo runs, create initial state matrices $\mathbf{X}$, and $\mathbf{\Xi}$ and compute the reduced order representations: mean, DO modes, and DO coefficients.
- Compute (or table look-up) $c(s)$ and $\nabla c(s)$ for all rays in all realizations.
- For s = 1:$\frac{RayLength}{\Delta s}$
  - Integrate the system of ODEs (Finite Difference or Runge-Kutta) to evolve mean, DO modes, and DO coefficients, separately.
  - Adjust DO modes and coefficients to ensure orthonormal basis is maintained.

- Identify reflections and modify DO modes, and DO coefficients.
- Compute (or table look-up) $c(s+1)$ and $\nabla c(s+1)$ for all rays in all realizations at the new $\mathbf{X}(s+1)$.

- End.

The above two implementations are further discussed and compared in [35]. Details about the computational schemes and implementation of the DO-Ray algorithms are also discussed in [35] including initialization, re-orthonormalization, and treatment of the surface and bottom boundary conditions.

IV. Applications

We now evaluate the DO-Ray algorithm in an uncertain deep sound channel sound speed field. We refer to [35] for additional stochastic ray tracing examples in uncertain ocean states.

Sound fixing and ranging (SOFAR) or deep sound channels (DSCs) are the result of specific ocean sound speed characteristics, principally a negative over a positive sound speed profile [45, 46]. Primarily observed in the mid-latitudes, having a minimum sound speed at deeper depths results in a condition where sound propagates in a duct, not interacting with the surface or bottom, making the only means of attenuation the absorption in the seawater [2]. In a deep sound channel, the acoustic energy of a source can be detected at ranges of several tens to hundreds of kilometers.

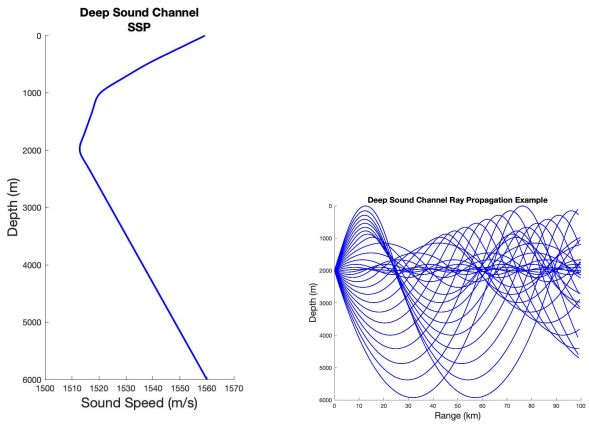

(a) SSP (b) Ray Trace

Fig. 2: Example of acoustic rays propagating in a deep sound channel with the acoustic source located at the deep sound channel axis (depth of minimum sound speed). Ray traces computed using 29 Rays evenly at evenly spaced angles between $\pm 14^{\circ}$, 2nd-order Runge-Kutta with a 1m step-size.

Consider a situation where the state of an upper column is highly variable due to abnormal weather events or abnormal seasonal variation. For underwater communication, detection and localization, it is of tactical significance to determine whether DSC propagation exists. A simple way of examining the existence and extent of the SOFAR channel would be to measure sound intensities at the ranges where we would expect the energy to focus. Here we consider that we have the means to measure signals produced only from about 10 km distances.

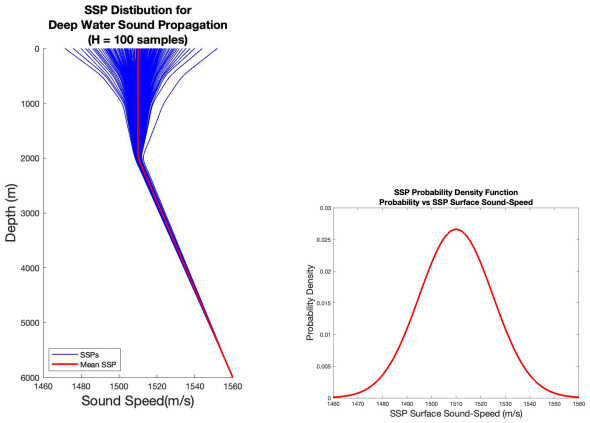

(a) SSP (b) Distribution

Fig. 3: From normal distribution of SSPs characterized by the surface sound-speed with a mean at 1500m/s (b) from which we can sample to obtain SSP realizations (a).

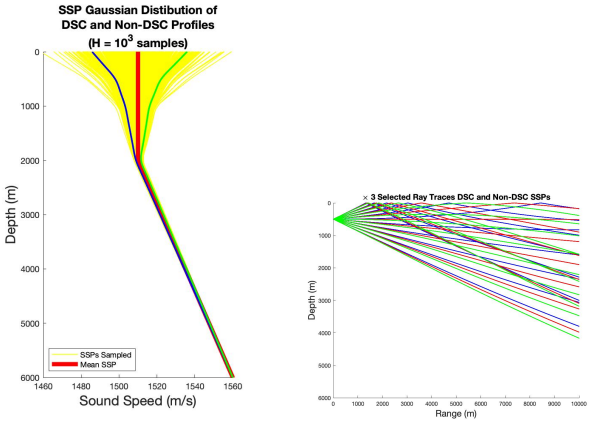

(a) SSP (b) Ray Trace

Fig. 4: (a) From our SSP distribution, we sample 1000 SSPs. (b) We computed the associated ray traces for the highlighted red (mean), green and blue SSPs. Only the green SSP environment of the three would result in a DSC. Ray traces computed using 11 Rays evenly at evenly spaced angles between $\pm 20^{\circ}$, 2nd-order Runge-Kutta with a 1m step-size.

In this scenario, we characterize the uncertainty as a Gaussian distribution of sound speed at the ocean surface, with sound-speed characteristics becoming more similar as depth increase (i.e. the SSP at deeper depths is unperturbed by surface events). In Figures 2 and 3, we show our sample distribution as well as computed ray traces for the mean SSP and two profiles closer to the edges of our Gaussian pdf. Only the SSP highlighted in

green would result in a DSC propagation environment where with the other two, over long distances the sound is refracted back to the surface. The variability in the ray propagation is still observed at shorter ranges, hence a measurement at this range could confirm the existence or non-existence of a DSC.

A. Capturing the Stochastic non-Gaussian Variability

Using the same computational schemes as those used for the Constant gradient SSPs, we computed ray trace ensembles with the stochastic DO-Ray equations and algorithm, then computed specified realizations within the ensemble using a deterministic implementation for comparison. Figure 5 provides a qualitative representation of the accuracy of the DO-Ray implementation. Again the ray traces are nearly indiscernible at this range scale as the DO-Ray overlays the deterministic solutions for all of the selected ocean SSPs.

B. Convergence with Number of DO Modes

For this distribution of SSPs the variability in ray paths result in positions $\sim$1000 m apart; with just a few modes, we can recreate realizations within $1-10$ m accuracy. In Figure 5, we showcase the first order convergence up to about 200 of the available 2002 DO modes where numerical errors begin to dominate the error.

V. Conclusions

Ocean acoustic computation is inherently challenging. This is compounded when attempting to perform stochastic computations with constrained resources. Innovative computational techniques and reduced order models exist with varying degrees of success. In this work, For the first time, we combined the Ray Method for acoustic computation with the stochastic Dynamically Orthogonal Equations (DO-Ray). We derived the stochastic DO-Ray differential equations, developed reduced-order algorithms, and demonstrated the ability to predict stochastic ray trace acoustics fields with the dynamically adaptive reduced-rank DO representation. We also discussed the use of local approximations to represent the nonlinear ray to sound-speed function transformation, including local sound-speed mean, sound-speed Taylor-Series, and sound-speed function. We applied DO-Ray to an idealized stochastic variable Deep Sound Channel and refer to [35] for other examples. Based on these results, we find that stochastic Ray-Trace field forecasting is feasible with a reduced rank-representation. The use of level-sets to capture all stochastic rays at once is also [47].

Future extensions of this work include applications in realistic 3D ocean acoustic environments, in addition to complementing this work with the use of level-sets to capture all stochastic rays at once [47]. Since ray trajectories are highly dependent on the ocean floor and surface characteristics, the ability to capture these variations in a

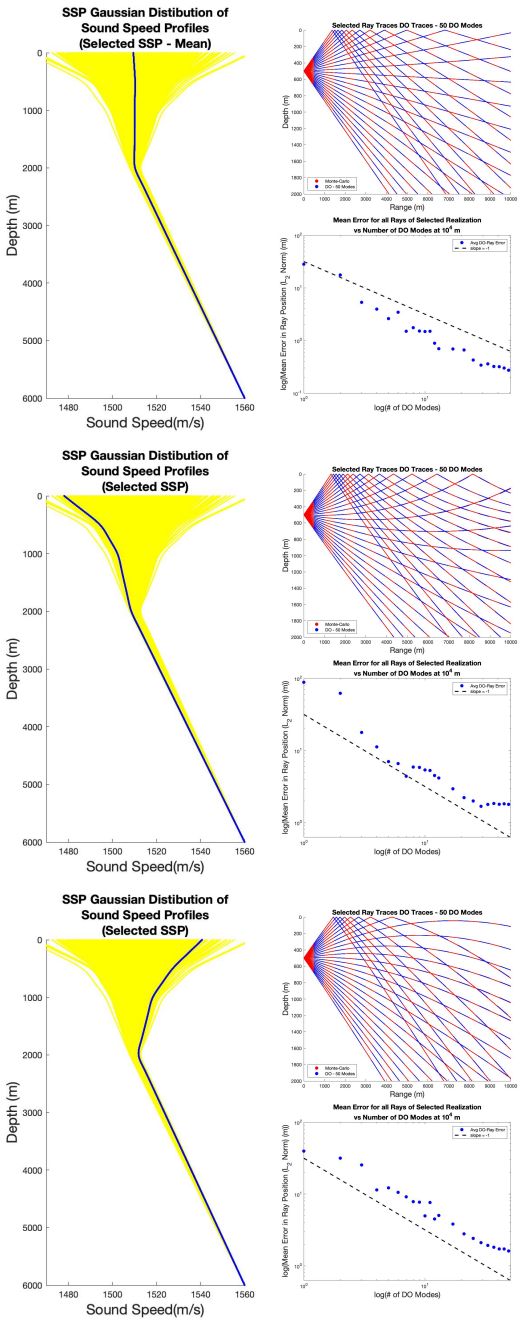

Fig. 5: Left panels: one ensemble member of sound speed distribution. Upper right panels: the DO-Ray computed ray trace (50 DO modes) overlaid with deterministic (Monte Carlo) traces. All traces computed using with 1001 Rays (26 Plotted) at evenly spaced angles between $\pm 20^\circ$ with a 1m step-size. The deterministic model uses 1st-order Forward Difference computational scheme. Lower right panels: convergence for selected realizations of the DO-Ray methodology with the deterministic solution. First order Convergence Line plotted for Reference. Deterministic traces computed using our deterministic model with 1001 Rays evenly at evenly spaced angles between $\pm 20^\circ$, 1st-order Forward Difference with a 1m step-size.

stochastic computation would advance the practical application to stochastic shallow water and under-ice acoustic predictions. Some potential approaches for incorporating the bathymetry and seabed uncertainties are proposed in [26, 27, 34], and adapting such approaches for the DO-Rays equations is an active research area.

Lastly, this methodology could be coupled with Bayesian data assimilation to improve the forecasting of the ocean and acoustic [3, 8, 48–51]. This offers advantages over classic tomography [45], matched field processing [52, 53], by allowing for the richer dynamics-based estimation of non-Gaussian statistics using stochastic differential physical laws. The results will be a more complete characterization of the coupled probability densities and a more powerful joint estimation of the ocean and acoustic states and their posterior uncertainties, combining multivariate observations with dynamical models based on principled information theory.

ACKNOWLEDGMENTS

We thank all members of the MSEAS group, past and present. We are grateful to the Office of Naval Research (ONR) for research support under grants N00014-19-1-2664 (Task Force Ocean: DEEP-AI) and N00014-19-1-2693 (IN-BDA) to the Massachusetts Institute of Technology. We thank the program managers Dr. Robert Headrick, Dr. Casey Church, Dr. Tom Drake, and Dr. Scott Harper for their inputs, and ADM John Richardson and RADM John Okon for their Task Force Ocean support.

REFERENCES

[1] L. M. Brekhovskikh and Y. Lysanov, *Fundamentals of Ocean Acoustics*. Springer, 1982.

[2] P. C. Etter, *Underwater acoustic modeling and simulation*. CRC press, 2018.

[3] P. F. J. Lermusiaux, "Uncertainty estimation and prediction for interdisciplinary ocean dynamics," *Journal of Computational Physics*, vol. 217, no. 1, pp. 176–199, 2006.

[4] P. F. J. Lermusiaux, C.-S. Chiu, G. G. Gawarkiewicz, P. Abbot, A. R. Robinson, R. N. Miller, P. J. Haley, Jr, W. G. Leslie, S. J. Majumdar, A. Pang, and F. Lekien, "Quantifying uncertainties in ocean predictions," *Oceanography*, vol. 19, no. 1, pp. 92–105, 2006.

[5] F. B. Jensen, W. A. Kuperman, M. B. Porter, and H. Schmidt, *Computational Ocean Acoustics*. Springer Science & Business Media, 2011.

[6] M. Rixen, P. F. J. Lermusiaux, and J. Osler, "Quantifying, predicting, and exploiting uncertainties in marine environments," *Ocean Dynamics*, vol. 62, no. 3, pp. 495–499, 2012.

[7] A. R. Robinson, P. Abbot, P. F. J. Lermusiaux, and L. Dillman, "Transfer of uncertainties through physical-acoustical-sonar end-to-end systems: A conceptual basis," in *Acoustic Variability, 2002*, N. G. Pace and F. B. Jensen, Eds. SACLANTCEN, K. Acad. Pr., 2002, pp. 603–610.

[8] A. R. Robinson and P. F. J. Lermusiaux, "Prediction systems with data assimilation for coupled ocean science and ocean acoustics," in *Proceedings of the Sixth International Conference on Theoretical and Computational Acoustics*, A. Tolstoy et al, Ed. World Scientific Publishing, 2004, pp. 325–342, refereed invited Keynote Manuscript.

[9] S. Finette, M. H. Orr, A. Turgut, J. R. Apel, M. Badiey, C.-s. Chiu, R. H. Headrick, J. N. Kemp, J. F. Lynch, A. E. Newhall *et al.*, "Acoustic field variability induced by time evolving internal wave fields," *The Journal of the Acoustical Society of America*, vol. 108, no. 3, pp. 957–972, 2000.

[10] P. F. J. Lermusiaux and C.-S. Chiu, "Four-dimensional data assimilation for coupled physical-acoustical fields," in *Acoustic Variability, 2002*, N. G. Pace and F. B. Jensen, Eds. Saclantcen: Kluwer Academic Press, 2002, pp. 417–424.

[11] J. Shorey, L. Nolte, and J. Krolik, "Computationally efficient monte carlo estimation algorithms for matched field processing in uncertain ocean environments," *Journal of Computational Acoustics*, vol. 2, no. 03, pp. 285–314, 1994.

[12] P. Gerstoft and C. F. Mecklenbräuker, "Ocean acoustic inversion with estimation of a posteriori probability distributions," *The Journal of the Acoustical Society of America*, vol. 104, no. 2, pp. 808–819, 1998.

[13] J. Xu, P. F. J. Lermusiaux, P. J. Haley Jr., W. G. Leslie, and O. G. Logutov, "Spatial and Temporal Variations in Acoustic propagation during the PLUSNet-07 Exercise in Dabob Bay," in *Proceedings of Meetings on Acoustics (POMA)*, vol. 4. Acoustical Society of America 155th Meeting, 2008, p. 11.

[14] M. E. G. D. Colin, T. F. Duda, L. A. te Raa, T. van Zon, P. J. Haley, Jr., P. F. J. Lermusiaux, W. G. Leslie, C. Mirabito, F. P. A. Lam, A. E. Newhall, Y.-T. Lin, and J. F. Lynch, "Time-evolving acoustic propagation modeling in a complex ocean environment," in *OCEANS - Bergen, 2013 MTS/IEEE*, 2013, pp. 1–9.

[15] P. F. J. Lermusiaux, C.-S. Chiu, and A. R. Robinson, "Modeling uncertainties in the prediction of the acoustic wavefield in a shelfbreak environment," in *Proceedings of the 5th International conference on theoretical and computational acoustics*, E.-C. Shang, Q. Li, and T. F. Gao, Eds. World Scientific Publishing Co., May 21-25 2002, pp. 191–200, refereed invited manuscript.

[16] P. F. J. Lermusiaux, A. R. Robinson, P. J. Haley, and W. G. Leslie, "Advanced interdisciplinary data assimilation: Filtering and smoothing via error subspace statistical estimation," in *Proceedings of The OCEANS 2002 MTS/IEEE conference*. Holland Publications, 2002, pp. 795–802.

[17] T. F. Duda, Y.-T. Lin, A. E. Newhall, K. R. Helfrich, J. F. Lynch, W. G. Zhang, P. F. J. Lermusiaux, and J. Wilkin, "Multiscale multiphysics data-informed modeling for three-dimensional ocean acoustic simulation and prediction," *Journal of the Acoustical Society of America*, vol. 146, no. 3, pp. 1996–2015, Sep. 2019.

[18] P. F. J. Lermusiaux, C. Mirabito, P. J. Haley, Jr., W. H. Ali, A. Gupta, S. Jana, E. Dorfman, A. Laferriere, A. Kofford, G. Shepard, M. Goldsmith, K. Heaney, E. Coelho, J. Boyle, J. Murray, L. Freitag, and A. Morozov, "Real-time probabilistic coupled ocean physics-acoustics forecasting and data assimilation for underwater GPS," in *OCEANS 2020 IEEE/MTS*. IEEE, Oct. 2020, pp. 1–9.

[19] P. F. J. Lermusiaux, P. J. Haley, Jr., C. Mirabito, W. H. Ali, M. Bhabra, P. Abbot, C.-S. Chiu, and C. Emerson, "Multi-resolution probabilistic ocean physics-acoustic modeling: Validation in the New Jersey continental shelf," in *OCEANS 2020 IEEE/MTS*. IEEE, Oct. 2020, pp. 1–9.

[20] S. Finette, "Embedding uncertainty into ocean acoustic

propagation models (l)," *The Journal of the Acoustical Society of America*, vol. 117, no. 3, pp. 997–1000, 2005.
[21] D. B. Creamer, "On using polynomial chaos for modeling uncertainty in acoustic propagation," *The Journal of the Acoustical Society of America*, vol. 119, no. 4, pp. 1979–1994, 2006.
[22] S. Finette, "A stochastic representation of environmental uncertainty and its coupling to acoustic wave propagation in ocean waveguides," *The Journal of the Acoustical Society of America*, vol. 120, no. 5, pp. 2567–2579, 2006.
[23] Y. Y. Khine, D. B. Creamer, and S. Finette, "Acoustic propagation in an uncertain waveguide environment using stochastic basis expansions," *Journal of Computational Acoustics*, vol. 18, no. 04, pp. 397–441, 2010.
[24] F. Gerdes and S. Finette, "A stochastic response surface formulation for the description of acoustic propagation through an uncertain internal wave field," *The Journal of the Acoustical Society of America*, vol. 132, no. 4, pp. 2251–2264, 2012.
[25] M. Branicki and A. J. Majda, "Fundamental limitations of polynomial chaos for uncertainty quantification in systems with intermittent instabilities," *Communications in mathematical sciences*, vol. 11, no. 1, pp. 55–103, 2013.
[26] W. H. Ali, M. S. Bhabra, P. F. J. Lermusiaux, A. March, J. R. Edwards, K. Rimpau, and P. Ryu, "Stochastic oceanographic-acoustic prediction and Bayesian inversion for wide area ocean floor mapping," in *OCEANS 2019 MTS/IEEE SEATTLE*, Oct. 2019, pp. 1–10.
[27] W. H. Ali and P. F. J. Lermusiaux, "Dynamically Orthogonal Narrow-Angle Parabolic Equations for Stochastic Underwater Sound Propagation," 2022, in preparation.
[28] A. Charous and P. F. J. Lermusiaux, "Dynamically orthogonal differential equations for stochastic and deterministic reduced-order modeling of ocean acoustic wave propagation," in *OCEANS 2021 IEEE/MTS*, Sep. 2021, pp. 1–7.
[29] T. P. Sapsis and P. F. J. Lermusiaux, "Dynamical criteria for the evolution of the stochastic dimensionality in flows with uncertainty," *Physica D: Nonlinear Phenomena*, vol. 241, no. 1, pp. 60–76, 2012.
[30] ——, "Dynamically orthogonal field equations for continuous stochastic dynamical systems," *Physica D: Nonlinear Phenomena*, vol. 238, no. 23–24, pp. 2347–2360, Dec. 2009.
[31] M. P. Ueckermann, P. F. J. Lermusiaux, and T. P. Sapsis, "Numerical schemes for dynamically orthogonal equations of stochastic fluid and ocean flows," *Journal of Computational Physics*, vol. 233, pp. 272–294, Jan. 2013.
[32] F. Feppon and P. F. J. Lermusiaux, "A geometric approach to dynamical model-order reduction," *SIAM Journal on Matrix Analysis and Applications*, vol. 39, no. 1, pp. 510–538, 2018.
[33] D. Subramani and P. F. J. Lermusiaux, "Probabilistic ocean predictions with dynamically-orthogonal primitive equations," 2022, in preparation.
[34] W. H. Ali and P. F. J. Lermusiaux, "Acoustics Bayesian inversion with Gaussianmixture models using the dynamically orthogonal field equations," 2022, in preparation.
[35] M. J. Humara, "Stochastic acoustic ray tracing with dynamically orthogonal equations," Master's thesis, Massachusetts Institute of Technology, Joint Program in App. Oc. Sc. and Eng., Cambridge, Massachusetts, May 2020.
[36] D. N. Subramani, T. Lolla, P. J. Haley, Jr., and P. F. J. Lermusiaux, "A stochastic optimization method for energy-based path planning," in *DyDESS 2014*, ser. LNCS, S. Ravela and A. Sandu, Eds., vol. 8964. Springer, 2015, pp. 1–12.
[37] D. N. Subramani and P. F. J. Lermusiaux, "Energy-optimal path planning by stochastic dynamically orthogonal level-set optimization," *Ocean Modeling*, vol. 100, pp. 57–77, 2016.
[38] D. N. Subramani, P. J. Haley, Jr., and P. F. J. Lermusiaux, "Energy-optimal path planning in the coastal ocean," *Journal of Geophysical Research: Oceans*, vol. 122, pp. 3981–4003, 2017.
[39] D. N. Subramani, Q. J. Wei, and P. F. J. Lermusiaux, "Stochastic time-optimal path-planning in uncertain, strong, and dynamic flows," *Computer Methods in Applied Mechanics and Engineering*, vol. 333, pp. 218–237, 2018.
[40] D. N. Subramani and P. F. J. Lermusiaux, "Risk-optimal path planning in stochastic dynamic environments," *Computer Methods in Applied Mechanics and Engineering*, vol. 353, pp. 391–415, Aug. 2019.
[41] A. Gupta, P. J. Haley, D. N. Subramani, and P. F. J. Lermusiaux, "Fish modeling and Bayesian learning for the Lakshadweep Islands," in *OCEANS 2019 MTS/IEEE SEATTLE*. Seattle: IEEE, Oct. 2019, pp. 1–10.
[42] M. M. Swezey, "Ocean acoustic uncertainty for submarine applications," Master's thesis, Massachusetts Institute of Technology, Department of Mechanical Engineering, Cambridge, Massachusetts, Jun. 2016.
[43] A. Phadnis, "Uncertainty quantification and prediction for non-autonomous linear and nonlinear systems," Master's thesis, Massachusetts Institute of Technology, Department of Mechanical Engineering, September 2013.
[44] S. Finette, "A stochastic response surface formulation of acoustic propagation through an uncertain ocean waveguide environment," *The Journal of the Acoustical Society of America*, vol. 126, no. 5, pp. 2242–2247, 2009.
[45] W. Munk, P. Worcester, and C. Wunsch, *Ocean acoustic tomography*. Cambridge university press, 2009.
[46] W. A. Kuperman and J. F. Lynch, "Shallow-water acoustics," *Physics Today*, vol. 57, no. 10, pp. 55–61, 2004.
[47] M. S. Bhabra and P. F. J. Lermusiaux, "Stochastic dynamically orthogonal acoustic wavefront equations," 2022, in preparation.
[48] T. Sondergaard and P. F. J. Lermusiaux, "Data assimilation with Gaussian Mixture Models using the Dynamically Orthogonal field equations. Part I: Theory and scheme." *Monthly Weather Review*, vol. 141, no. 6, pp. 1737–1760, 2013.
[49] ——, "Data assimilation with Gaussian Mixture Models using the Dynamically Orthogonal field equations. Part II: Applications." *Monthly Weather Review*, vol. 141, no. 6, pp. 1761–1785, 2013.
[50] T. Lolla and P. F. J. Lermusiaux, "A Gaussian mixture model smoother for continuous nonlinear stochastic dynamical systems: Theory and scheme," *Monthly Weather Review*, vol. 145, pp. 2743–2761, Jul. 2017.
[51] ——, "A Gaussian mixture model smoother for continuous nonlinear stochastic dynamical systems: Applications," *Monthly Weather Review*, vol. 145, pp. 2763–2790, Jul. 2017.
[52] S. E. Dosso, "Quantifying uncertainty in geoacoustic inversion. i. a fast gibbs sampler approach," *The Journal of the Acoustical Society of America*, vol. 111, no. 1, pp. 129–142, 2002.
[53] A. B. Baggeroer, W. A. Kuperman, and P. N. Mikhalevsky, "An overview of matched field methods in ocean acoustics," *IEEE Journal of Oceanic Engineering*, vol. 18, no. 4, pp. 401–424, 1993.